

Active Linear Quadratic Gaussian Secondary Suspension Control of Flexible Bodied Railway Vehicle

Kaushalendra K. Khadanga, Lee Hee Hyol

Abstract—Passenger comfort has been paramount in the design of suspension systems of high speed cars. To analyze the effect of vibration on vehicle ride quality, a vertical model of a six degree of freedom railway passenger vehicle, with front and rear suspension, is built. It includes car body flexible effects and vertical rigid modes. A second order linear shaping filter is constructed to model Gaussian white noise into random rail excitation. The temporal correlation between the front and rear wheels is given by a second order Pade approximation. The complete track and the vehicle model are then designed. An active secondary suspension system based on a Linear Quadratic Gaussian (LQG) optimal control method is designed. The results show that the LQG control method reduces the vertical acceleration, pitching acceleration and vertical bending vibration of the car body as compared to the passive system.

Keywords—Active suspension, bending vibration, railway vehicle, vibration control.

I. INTRODUCTION

A typical railway vehicle has two bogies that are connected to the car body by the secondary suspensions. Each bogie has two-wheel sets that are connected by primary suspensions. With increase in railway vehicle speeds, the vehicles dynamic performances are negatively affected. Since secondary suspension directly influences passenger ride comfort, it must be modified to compensate for the deteriorated dynamic behavior. To improve ride comfort, it is also important to know the different vibration modes of the car body. The vibrations are mainly caused by track irregularities that are transmitted up to the car body. Good ride comfort is achieved by suppressing these vibrations.

The car body vibration modes are of two types: rigid and flexible. The rigid mode vibrations are the bounce, pitch and roll. These vibrations are in low frequency zone which is around 1 Hz. The flexible modes are bending and twisting deformations of the car body, the first flexible modes lie in the range of 8-15 Hz [5]. As speed of railway vehicle goes up, lighter vehicle designs like aluminum bodies are being preferred, which are more flexible with greater structural vibrations than rigid design bodies. Hence suppression of

vibration of flexible modes is necessary besides rigid modes to improve ride comfort of passengers.

II. BACKGROUND

A railway vehicle is a large, complex and dynamic system. In the beginning, railway vehicles had only mechanical systems. But today, railway vehicles are very much dependent on electronics, computer and digital processing [1]. It becomes more complex when the flexibility of the components is considered.

Active secondary suspension is the effective approach for vibration control to improve ride comfort [3]. An active secondary suspension system consists of actuators, sensors and a specific control law which generates the force demand for the actuator. Ride quality evaluation has been studied as a weighted power spectral density of the car body acceleration [2]. Rigid-body models are not suitable enough to predict ride comfort accurately. Calbom has studied the effect of car body flexibility on ride quality and vehicle dynamics [4], [5].

In this paper, a 6 degree of freedom vertical half car Shinkansen type passenger vehicle is considered. The car body is modelled as a simple uniform Euler Bernoulli beam supported on secondary suspension as shown in Fig. 1. The power spectral densities for the lateral alignment and vertical profile are considered. Random rail excitation is used in terms of white noise which is fed into a second order linear shaping filter [6], [7]. Time delay between the wheels is considered by making use of Laplacian operators and second order Pade approximation [8]. A control law using LQG is designed which includes a Kalman Filter. It is proposed to design the active suspension to suppress not only the rigid body vibrations but also the first bending mode vibrations of the rail vehicle. The various physical parameters of the passenger coach as shown in Table I belong to a class of E6 series of Shinkansen train.

III. VEHICLE MODELLING

Fig. 1 shows the model used in this paper. It consists of a flexible passenger coach suspended by the front and rear bogies. The bounce and pitch motions of the car body and the two bogies have been considered. In addition, flexible bending modes of the car body are also considered. The vertical movements of the wheel are assumed to be same as track irregularities.

Kaushalendra K. Khadanga is a master's student with Waseda University, Graduate School of Information, Production and Systems, Kitakyushu, Japan (corresponding author, phone: 080-9987-2150; e-mail: kaushalkishore@akane.waseda.jp).

Lee Hee Hyol is a Professor at Waseda University, Graduate School of Information, Production and Systems, Kitakyushu, Japan (e-mail: hlee@waseda.jp).

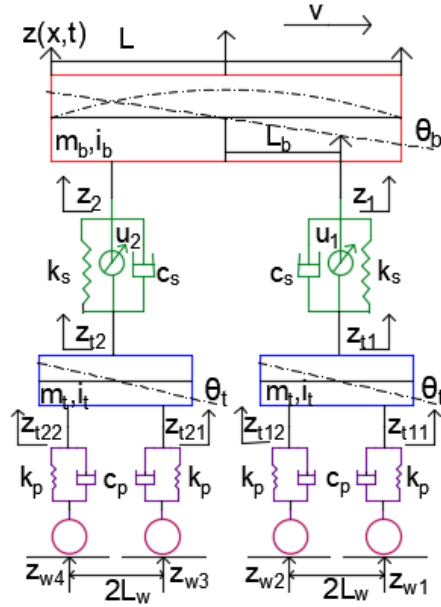


Fig. 1 Six Degrees of Freedom Half car Model

The following are the important symbols used in this paper.

TABLE I
IMPORTANT SYMBOLS

M_b, M_t	mass of car body and bogies
I_b, I_t	pitch moment of inertia of car body and bogies
C_s, C_p	damping coefficient of primary and secondary
K_s, K_p	spring stiffness of primary and secondary
L, L_w, L_b	length of coach, half of wheel base, distance from c.g of car body and centre of bogie
ω_m, ξ_m	natural frequency, damping percent
$EI, \mu I, f$	car body bending moment, internal viscous damping coefficient, density

TABLE II
SYSTEM PARAMETERS OF CAR BODY AND BOGIE

Parameter	Value	Parameter	Value
M_b	26,000 kg	K_p	2,370,000 N/m
M_t	7,000 kg	L	24.5 m
I_b	2,345,778 kg m ²	L_w	1.25 m
I_t	7,865 kg m ²	L_b	8.75 m
C_s	113,000 Ns/m	EI	2.18E9 N m ²
C_p	78,400 Ns/m	μI	7.4E5 N/(m/s)
K_s	355,900 N/m		

A. Car Body Model

The equation of the vehicle body is assumed as a partial differential equation of Euler Bernoulli Beam with free-free end conditions [9], [10]. The vertical displacements of the car body $z(x,t)$ as a function of the horizontal axis and time is given by

$$EI \frac{\partial^4}{\partial x^4} z(x, t) + \mu I \frac{\partial^5}{\partial t \partial x^4} z(x, t) + f \frac{\partial^2}{\partial t^2} z(x, t) = \sum_{i=1}^2 f_i(t) \delta(x - l_i) \quad (1)$$

The first term in (1) is the bending rigidity of the body, the second term is the damping of the body and the third term is that of inertia. $f_1(t)$ is the front suspension force and $f_2(t)$ is the

rear suspension force. The displacement at each point is a summation of natural mode solutions. The partial differential equation (1) is solved using variable separation method. When the rigid modes are included with the flexible modes in $Z(x, t)$, the first mode is the bounce of the rigid mode and its shape function is taken as $Y_1(x) = 1$. The second mode is the pitch and its shape function is $Y_2(x) = (x-l/2)$.

$$Z(x, t) = \sum_{m=1}^N Y_m(X) q_m(t) = z_b(t) + (x - l/2) \theta_b(t) + \sum_{m=3}^N Y_m(X) q_m(t) \quad (2)$$

The first term on the right-hand side is the vertical rigid body mode. The second term is the pitch motion. The third term is the summation of the bending modes of the vehicle body. The shape function and the modal coordinate of the m^{th} mode are $Y_m(X)$ and $q_m(t)$ respectively. For $m \geq 3$, the shape functions are given by

$$Y_m(X) = \cos h \beta_m x + \cos \beta_m x - \frac{\cos h \lambda_m x - \cos \lambda_m x}{\sin h \lambda_m x - \sin \lambda_m x} (\sin h \beta_m x + \sin \beta_m x) \quad (3)$$

where $\cos h(\beta_m L) + \cos \beta_m L = 1$ and $\beta_m L = \lambda_m$

By substituting (2) into (1) and integrating along the length of the car body and assuming that the damping function to be very small and the eigenfunction of each mode to be orthogonal, the ordinary differential equation of each motion is obtained as follows:

$$M_b \frac{d^2}{dt^2} Z_b = f_1(t) + f_2(t) : m=1 \quad (4)$$

$$I_b \frac{d^2}{dt^2} \theta_b = f_1(t) L_b - f_2(t) L_b : m=2 \quad (5)$$

$$\ddot{q}_m(t) + \frac{\mu I \beta_m^4}{\rho} \dot{q}_m(t) + \frac{EI \beta_m^4}{\rho} q_m(t) = \frac{Y_m(l_1)}{M_b} f_1(t) + \frac{Y_m(l_2)}{M_b} f_2(t) : m = 3, 4, \dots, n \quad (6)$$

Let $\frac{EI \beta_m^4}{\rho} = \omega_m^2$ and $\frac{\mu I \beta_m^4}{\rho} = 2\xi_m \omega_m$, (6) becomes

$$\ddot{q}_m(t) + 2\xi_m \omega_m \dot{q}_m(t) + \omega_m^2 q_m(t) = \frac{Y_m(l_1)}{M_b} f_1(t) + \frac{Y_m(l_2)}{M_b} f_2(t), \quad m = 3, 4, \dots, n \quad (7)$$

Although a total of 33 modes within 5-20 Hz are known like car body bending and torsion, diagonal torsion and roof/side/floor walls vibration, experimentally, it is seen that the first vibration mode which is the bending mode has the maximum influence on the car body dynamic behavior. Hence, we neglect the modes higher than the first bending mode ($M=3$). Considering the first bending mode alone, $\beta_3 L = 4.73$, or $\beta_3 = 4.73/L = 0.54$.

B. Modelling of Connecting Forces

Let us now determine the mathematical expressions for transmission forces at the car body supporting points at secondary suspensions. The front suspension forces $f_1(t)$ and the rear suspension force $f_2(t)$ are the linear combination of the forces due to the spring, damper, deflection due to bending,

deflection due to pitching and the force of actuators.

$$f_1(t) = -K_s [(z_1 - z_{11}) - L_b \theta_b + Y_1 q_1] - C_s [(\dot{z}_1 - \dot{z}_{11}) - L_b \dot{\theta}_b + Y_1 \dot{q}_1] - U_1 \quad (8)$$

$$f_2(t) = -K_s [(z_2 - z_{12}) - L_b \theta_b + Y_2 q_2] - C_s [(\dot{z}_2 - \dot{z}_{12}) - L_b \dot{\theta}_b + Y_2 \dot{q}_2] - U_2 \quad (9)$$

Using (4), (5), (7)-(9), the equations of motion of the car body becomes:

$$M_b \ddot{z}_b = K_s(z_{12} - z_2) + K_s(z_{11} - z_1) + C_s(\dot{z}_{12} - \dot{z}_2) + C_s(\dot{z}_{11} - \dot{z}_1) - U_2 - (Y_1 + Y_2)K_s q_1 - (Y_1 + Y_2)C_s \dot{q}_1 \quad (10)$$

$$I_b \ddot{\theta}_b = -K_s(z_1 - z_{11})L_b - C_s(\dot{z}_1 - \dot{z}_{11})L_b + K_s(z_2 - z_{12})L_b - C_s(\dot{z}_2 - \dot{z}_{12})L_b - L_b U_1 + L_b U_2 + L_b(Y_2 - Y_1)K_s q_1 - L_b(Y_2 - Y_1)C_s \dot{q}_1 \quad (11)$$

The vibration equations of the two bogies of the passenger coach can be deduced using Newton's second law of motion:

$$M_1 \ddot{z}_{11} = K_s(z_1 - z_{11}) + C_s(\dot{z}_1 - \dot{z}_{11}) - K_p(z_{112} - z_{w2}) - K_p(z_{111} - z_{w1}) - C_p(\dot{z}_{111} - \dot{z}_{w1}) - C_p(\dot{z}_{112} - \dot{z}_{w2}) + U_1 + Y_1 K_s q_1 + Y_1 C_s \dot{q}_1 \quad (12)$$

$$I_1 \ddot{\theta}_{11} = -K_p(z_{111} - z_{w1})L_w - C_p(\dot{z}_{111} - \dot{z}_{w1})L_w + K_p(z_{112} - z_{w2})L_w + C_p(\dot{z}_{112} - \dot{z}_{w2})L_w \quad (13)$$

$$M_1 \ddot{z}_{12} = K_s(z_2 - z_{12}) + C_s(\dot{z}_2 - \dot{z}_{12}) - K_p(z_{121} - z_{w3}) - K_p(z_{122} - z_{w4}) - C_p(\dot{z}_{121} - \dot{z}_{w3}) - C_p(\dot{z}_{122} - \dot{z}_{w4}) + U_2 + Y_2 K_s q_1 + Y_2 C_s \dot{q}_1 \quad (14)$$

$$I_1 \ddot{\theta}_{12} = -K_p(z_{121} - z_{w3})L_w - C_p(\dot{z}_{121} - \dot{z}_{w3})L_w + K_p(z_{122} - z_{w4})L_w + C_p(\dot{z}_{122} - \dot{z}_{w4})L_w \quad (15)$$

C. State Space Formulation

Three different patterns of state space design were tried for selection of state variables. In the first design, the vertical and angular displacement of the car body and their derivatives were considered as state variables. The front and rear vertical displacements of each bogie and their derivatives were also taken as state variables. But this design was not controllable and observable. Hence it was discarded.

In the second design, in addition to the vertical displacement and angular displacement and the corresponding velocities of the car body, the vertical and angular displacement and the corresponding velocities of each bogie were considered as independent state variables. However, this also had similar problems as the first design with respect to the controllability and observability.

In the third design, the vertical displacements of the front and rear portions of the car body and the bogies and their corresponding derivatives are considered as independent state variables. The angular displacement of the car body and the bogies were determined by algebraic relations. This design is controllable and observable. Hence this was chosen for further analysis. The state variables are shown in Table III.

The equations of motion as derived in (7) and (10)-(15) are put in state space form using the state variables shown in Table III. z is the exogenous output vector. u_1, u_2 are the control input forces.

TABLE III
STATE VARIABLES

$z_1 = x_1$	$z_{122} = x_6$	$\dot{z}_{121} = x_{11}$
$z_2 = x_2$	$\dot{z}_1 = x_7$	$\dot{z}_{122} = x_{12}$
$z_{111} = x_3$	$\dot{z}_2 = x_8$	$q_1(t) = x_{13}$
$z_{112} = x_4$	$\dot{z}_{111} = x_9$	$\dot{q}_1(t) = x_{14}$
$z_{121} = x_5$	$\dot{z}_{112} = x_{10}$	

$$\begin{aligned} \dot{x} &= Ax + B_1 \dot{z}_w + B_2 z_w + B_3 u \\ Y &= C_1 x \\ z &= C_2 x + Du \end{aligned} \quad (16)$$

where,

$$\begin{aligned} x &= [x_1, x_2, x_3 \dots x_{10}, x_{11}, x_{12}, q(t), \dot{q}(t)]^T \\ \dot{z}_w &= [\dot{z}_{w1}, \dot{z}_{w2}, \dot{z}_{w3}, \dot{z}_{w4}]^T \\ z_w &= [z_{w1}, z_{w2}, z_{w3}, z_{w4}]^T \\ u &= [u_1, u_2]^T \end{aligned}$$

D. Stochastic Rail Track Input

Random nature of man-made surfaces like rail tracks has been investigated by the researchers in the past [6]. They found that a good approximation of the unevenness can be realized by a stationary random Gaussian process given by its Power Spectral Density (PSD). The PSD for both lateral alignment and vertical profile is given by:

$$S_v(\Omega) = \frac{A_v \Omega_c^2}{(\Omega^2 + \Omega_r^2)(\Omega^2 + \Omega_c^2)}$$

where Ω is the spatial frequency or wave number in cycle/m, A_v is the rail roughness coefficient, Ω_r and Ω_c are the cut-off frequencies [11]. The equation is in spatial domain. So, it is converted into time domain by using the relationship between PSD and velocity. The Federal Railroad Administration classifies the track quality into 9 categories and the values of A_v , Ω_c , Ω_r have been taken for a track of class 6 [12]. From the transfer function, the state space form is obtained using Laplace inverse transformation. This is for the first wheel with white noise as input. A time delay function for remaining three wheels is used which is as

$$Z_{wi}(t) = Z_{w1}(t - \zeta_i), \quad i = 1, 2, 3, 4 \quad (17)$$

where $\zeta_1 = 0$, $\zeta_2 = 2 L_w/V$, $\zeta_3 = 2 L_b/V$, $\zeta_4 = (2 L_w + 2 L_b)/V$. Using the second order Pade approximation, we obtain the complete state space form of the stochastic rail input for all the wheels. Here γ is the disturbance in terms of Gaussian white noise

$$\begin{aligned} \dot{x}_w &= A_w x_w + B_w \gamma \\ z_w &= C_w x_w \end{aligned} \quad (18)$$

E. State Space of Complete Train System

Now we have two different set of equations, one for the vehicle dynamics equations and the other for the rail track excitation equations. By algebraic manipulations, these two systems of equations (16) and (18) are now combined to form the complete train system of equations (19).

$$\begin{aligned} \frac{d}{dt} \tilde{x} &= \tilde{A} \tilde{x} + \tilde{B}_1 Y(t) + \tilde{B}_2 u \\ Y &= \tilde{C} \tilde{x} \\ z &= \tilde{C}_2 \tilde{x} + Du \end{aligned} \quad (19)$$

$$u = -K_r \hat{x} \quad (21)$$

For the regulator, the objective is to minimize the quadratic cost function J , which is defined as

$$J = \int (z^T Q z + u^T R u) dt \quad (22)$$

Q and R are the weighting matrices. They define the trade-off between the regulation performance and control effort. The simulation is done in MATLAB/Simulink.

where,

$$\begin{aligned} \tilde{x} &= [X \ X_w]^T \quad \tilde{A} = \begin{bmatrix} A & B_1 C_w A_w + B_2 C_w \\ 0 & A_w \end{bmatrix} \\ \tilde{B}_1 &= \begin{bmatrix} B_1 C_w B_w \\ B_w \end{bmatrix} \quad \tilde{B}_2 = \begin{bmatrix} B_3 \\ 0 \end{bmatrix} \quad \tilde{C} = \begin{bmatrix} C_1 \\ 0 \end{bmatrix} \end{aligned}$$

IV. DESIGN OF LQG CONTROLLER

LQG controller is used to determine the controller for the secondary suspension. The LQG controller is a combination of Linear Quadratic Regulator and Kalman filter. Since in practice, we do not have access to full state in a system, we determine a few measurements, denoted by Y . The vehicle model given by (19) is assumed to have an artificial sensor noise θ , as

$$Y = \tilde{C} \tilde{x} + \theta$$

The covariance structure is assumed to be as shown:

$$E\{\gamma\gamma^T\} = 1, E\{\gamma\theta^T\} = 0, E\{\theta\theta^T\} = \rho I$$

The operator E gives the expected value. The covariance ρ is assumed to have a value less than 1. Kalman filter is an optimum full state estimator that gives \hat{x} . The controllability and observability conditions have been satisfied.

The LQG design is based on separation principle where the Kalman filter and LQR are independently determined. By changing the sensor noises covariances and disturbance noise covariances, different sets of results can be obtained. By solving algebraic ricatti equation, Kalman filter gain K_f is calculated to find the estimate of the state \hat{x} given by \hat{x} .

$$\frac{d}{dt} \hat{x} = \tilde{A} \hat{x} + \tilde{B}_1 u + K_f (Y - \tilde{C} \hat{x}) \quad (20)$$

By solving another algebraic Ricatti equation the regulator gain K_r is calculated to find the control force which uses \hat{x} which is the estimate obtained from (20).

V. SIMULATION

The root mean square (RMS) response of the passive suspension and the LQG designed active suspension in terms of the vertical acceleration, pitching acceleration and the suspension travels of the front and rear bogies are tabulated in Table III.

TABLE III
RMS RESPONSES

Output	Passive	Active	Performance
Vertical Acceleration	2.4569	2.0696	16%
Pitching Acceleration	0.2810	0.2006	28.6%
Front Suspension Travel	0.0278	0.0165	40.6%
Rear Suspension Travel	0.0264	0.0258	2%

As per Table III, the vertical acceleration and pitching acceleration have shown an improvement in the RMS values in active suspension as compared to passive suspension by 16% and 28.6% respectively. The table shows that although the front secondary suspension travel is improved in active suspension by 40.6%, the rear secondary suspension travel is just improved by 2% which is a tradeoff. Flexible choices of weighting matrices Q and R gives different performance indices to compare the performance of the controller. The time series plots of the vertical acceleration and pitching acceleration have also been drawn in Figs. 2 and. 3, respectively. The plot shows improvement in the vertical acceleration and pitching accelerations in active suspension over passive suspension.

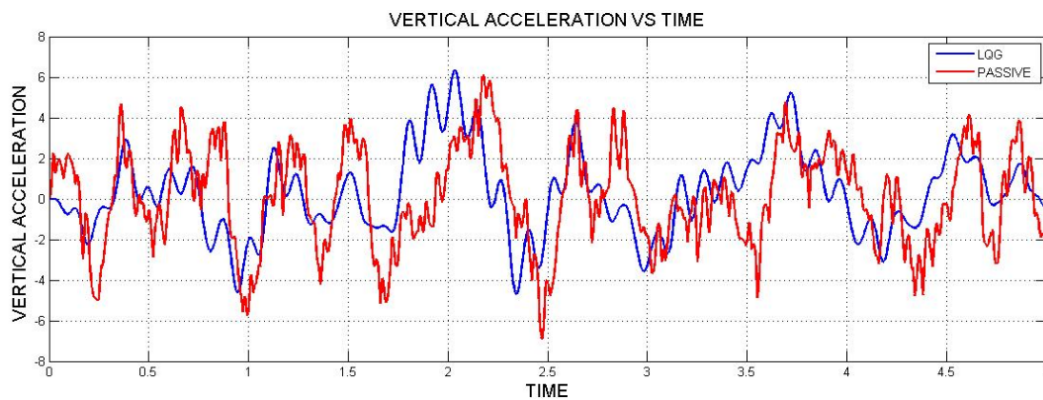


Fig. 2 Time Series Plot of Vertical Acceleration

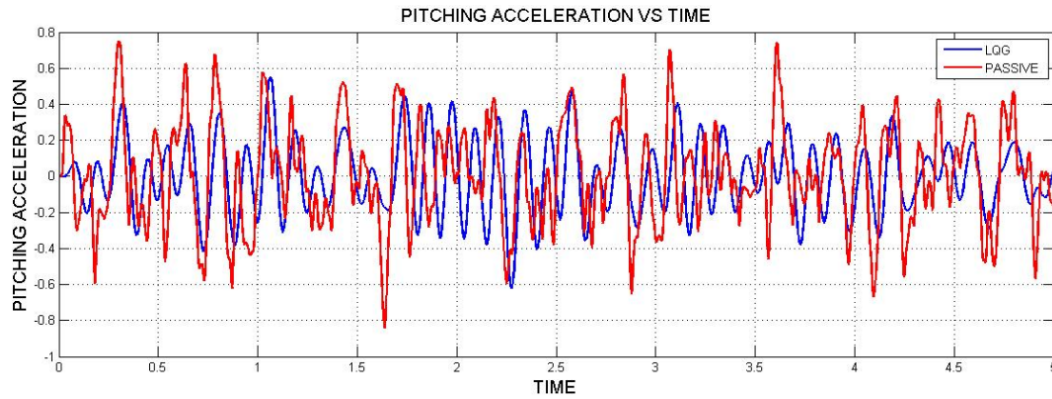


Fig. 3 Time Series Plot of Pitching Acceleration

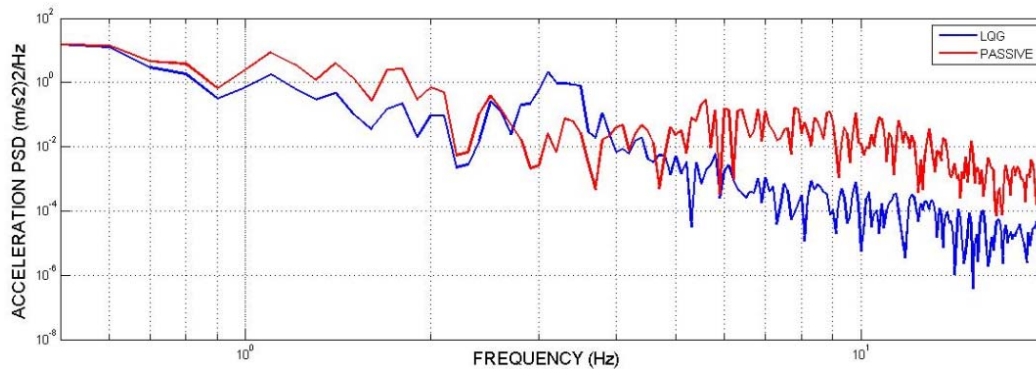


Fig. 4 Acceleration PSD of the Centre of Car Body

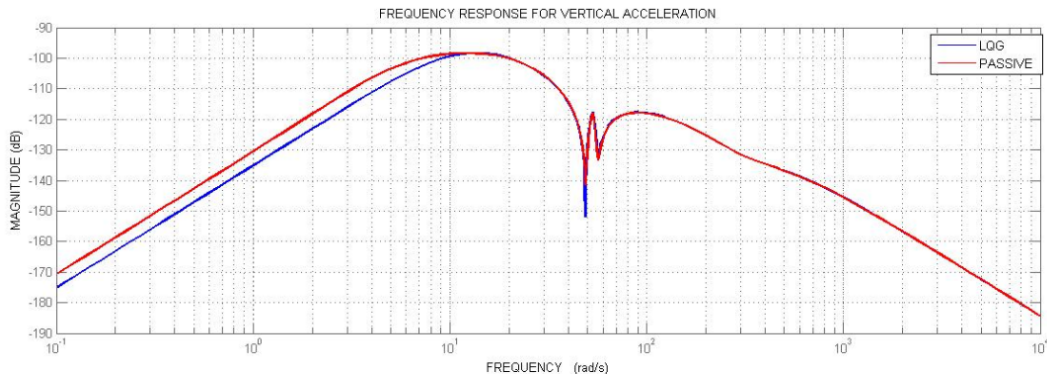


Fig. 5 Frequency Response for Vertical Acceleration

All study indicates that car body vertical bending mode significantly influences the vertical ride comfort. The car body has a natural frequency of 8-8.5 Hz in the first bending mode. The vibration acceleration PSD graph shows that the overall vibration decreases in the frequency range of 5-12 Hz. At the first bending mode frequency also, the peak is reduced in the LQG active suspension. This is seen in Fig. 4.

Mode plots also give us a many information regarding the magnitude of the frequency response in dB. They are shown in Figs. 5 and 6.

In Fig. 5, the frequency response of vertical acceleration is reduced in LQG system as compared to the one in passive system, up to 10 Hz. This is good as humans are sensitive to vertical vibration in the range of 4-10 Hz. Fig. 6 also says that frequency response of pitching acceleration is reduced in range of 5-12 Hz.

The RMS values of the control forces U_1 and U_2 for the two secondary suspension actuators have also been determined as shown in Table IV. It shows that required control effort is not large.

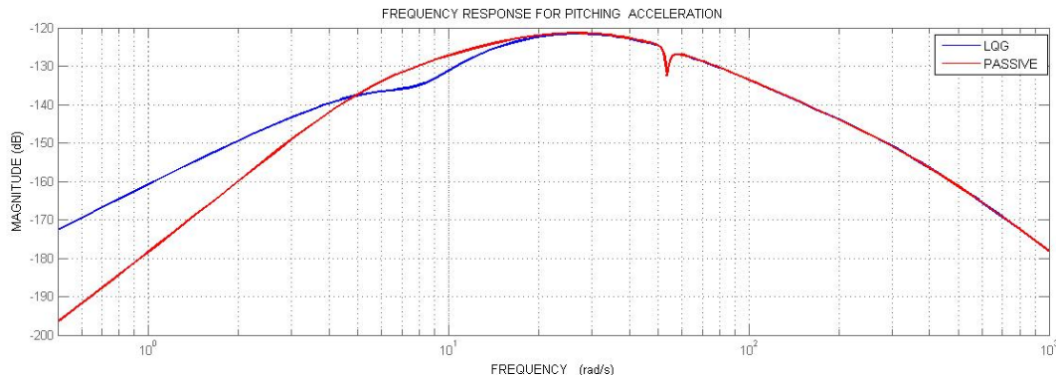


Fig. 6 Frequency Response for Pitching Acceleration

TABLE IV
CONTROL FORCES

Output	RMS Value	Maximum value
Front Actuator Force U_1	7892.2N	15.7kN
Rear Actuator Force U_2	19060N	37.5kN

From the foregoing paragraphs, it is seen that the rigid body peaks at low frequency of 1-2 Hz and first bending mode peak of 8.5 Hz have been considerably reduced in the LQG based active suspension system.

VI. CONCLUSION

In this work, an active secondary suspension system for a flexible bodied railway vehicle is designed using LQG. Random rail excitations at the front wheel are modelled as a linear shape filter. The time delay between the wheels is modelled by making use of Pade's approximation. Performance parameters were established in time series and frequency domain as well as PSD curves. The LQG scheme improved the ride comfort over a passive system. As it is not practical to measure all the states in a running system, hence LQG system is more favorable among others in industrial systems.

The effect of more complex modes of vibration of the car body is necessary for detailed design, but the characteristic of those modes is vehicle specific. Hence a simpler design gives a better general understanding.

When analyzing the car body bending mode vibrations and its effect on the ride comfort, a finite element model of the car body could be built in ADAMS/rail or SIMPACK. A detailed and accurate analysis could be done in this software.

Parametric time varying or time independent uncertainties are always there in any dynamic system. Load varies from time to time. The performance of springs, dampers and actuators vary with time either linearly or non-linearly. The LQG system described is a highly parametric dependent system. The effect of uncertainties on the LQG design, in other words, the robustness issue of LQG has not been studied in detail here. It needs to be analyzed to cater uncertainties.

REFERENCES

- [1] A.G Zolotas, R. M. Goodall, "Modelling and control of railway vehicle

suspensions", *Mathematical Methods for Robust and Non-Linear Control: Springer*, New York, pp 373-412.

- [2] R.H Fries and B.M. Coffey, "A state-space approach to the synthesis of random vertical and crosslevel rail irregularities," *Journal of Dynamic Systems, Measurements and Control*, vol. 112, pp. 83-87, Mar 1990.
- [3] A. Orvnas, "Active Secondary Suspension in Trains: A literature Survey. (Unpublished work style)," unpublished.
- [4] P. Carlbom, "Car body and Passengers in Rail Vehicle Dynamics," doctoral dissertation, Royal Institute of Technology, Sweden, 2000.
- [5] P. Carlbom, "Combining MBS with FEM for rail vehicle dynamics analysis," *Multibody Systems Dynamics*, vol. 6, pp. 291-300, 2001.
- [6] W.O. Schiehlen, "White noise excitation of road vehicle structures", *Sadhana*, vol. 31, part 4, pp 487-503, Aug 2006.
- [7] W.O. Schiehlen, "Dynamics of High Speed Vehicles", *International Centre for Mechanical Sciences*, Springer-Verlag wein GmbH, pp 13-60, 1982.
- [8] J. Zhou, G. Shen, H. Zhang and L. Ren, "Application of Modal Parameters on Ride Quality Improvement of Railway Vehicles," *Vehicle Systems Dynamics*, vol. 46, pp 629-641, Supplement, 2008.
- [9] L. Jacobsen, R. Ayre, "Engineering Vibrations", McGraw Hill Series in Mechanical Engineering, McGrawHill, pp 455-496, 1958.
- [10] S. Rao, "Mechanical Vibrations", Prentice Hall, pp 721-739, 2011.
- [11] P.O. Detwiler, M.L. Nagurka, "Track geometry modelling for rail vehicle studies", *Dynamic Systems: Modelling and Control*, ASME DSC-vol 1, pp 325-331, 1985.
- [12] A. Hamid, K. Rasmussen, M. Baluja, T.L. Yang., "Analytical Descriptions of Track Geometry Variations", office of Research and Development, US Department of Transportation, Federal Railroad Administration, 1983.